AGU PUBLICATIONS

Geochemistry, Geophysics, Geosystems

RESEARCH ARTICLE
10.1002/2017GC006804

Key Points:
- Increasing %TOC values in the Southeastern Arabian Sea since mid-Holocene
- These values are result of better preservation and not higher productivity
- South Asian Summer Monsoon declined since mid-Holocene

Supporting Information:
- Figure S1
- Figure S2
- Table S1

Correspondence to:
M. Tiwari,
manish@ncaor.gov.in

Citation:
Nagoji, S. S., and M. Tiwari (2017), Organic carbon preservation in Southeastern Arabian Sea sediments since mid-Holocene: Implications to South Asian Summer Monsoon variability, *Geochem. Geophys. Geosyst.*, *18*, doi:10.1002/2017GC006804.

Received 6 JAN 2017
Accepted 31 JUL 2017
Accepted article online 14 AUG 2017

Organic carbon preservation in Southeastern Arabian Sea sediments since mid-Holocene: Implications to South Asian Summer Monsoon variability

Siddhesh S. Nagoji[1] and Manish Tiwari[1]

[1]National Centre for Antarctic and Ocean Research, Vasco-da-Gama, Goa, India

Abstract The earlier studies show a contrasting long-term trend of the South Asian Summer Monsoon (SASM) after attaining the precessional forcing induced mid-Holocene maximum. The increasing total organic carbon (TOC) concentration of marine sediments in the Southeastern Arabian Sea (SEAS) has been interpreted to imply strengthening SASM since mid-Holocene by a few studies. However, TOC concentration is also influenced by redox conditions, sedimentation rate, and an influx of terrigenous matter depending on the regional settings. So, it needs to be ascertained whether the TOC concentration of the sediments in the SEAS is a signal of productivity related to the SASM strength or preservation. Therefore, we studied multiple proxies (TOC, total nitrogen, atomic C/N, $\delta^{13}C_{org}$, $CaCO_3$, and major and trace elements concentration) for determining the productivity, redox conditions, detrital supply, and provenance in a sediment core from the upper continental slope of the SEAS spanning the past ~4700 years at centennial scale resolution. The present study shows that the observed increase in the TOC values since the mid-Holocene is a result of better preservation caused by increased sedimentation rate and enhanced reducing conditions. We further show that the SASM has been declining since mid-Holocene after attaining a precession-forced maximum, which corroborates the earlier model ensemble studies.

1. Introduction

The South Asian Summer Monsoon (SASM) variability on different timescales is an intense area of research due to its influence on the life and economic conditions of billions of people. Despite a large number of studies to decipher its past variability, the consensus has not yet evolved for the SASM variability after attaining the orbital forcing induced mid-Holocene (~5–6 ka) maximum. General circulation model ensemble [*Chevalier et al.*, 2017] as well as paleo-proxy data [*deMenocal et al.*, 2000; *Russell et al.*, 2003; *Weldeab et al.*, 2007] show that the northern African summer monsoon was stronger than present during the mid-Holocene due to the higher amount of heat received by the northern tropics during summer because of the precessional forcing. Likewise, model ensemble studies have also proposed stronger than present mid-Holocene East Asian Summer Monsoon (EASM) [*Jiang et al.*, 2013] and the SASM [*Joussaume et al.*, 1999]. Present day orbital configuration is of precession maximum implying perihelion during northern hemisphere winters. Therefore, the northern tropics would receive lower insolation during summer than mid-Holocene leading to decreasing monsoon intensity since then. But, based on various proxy records from different regions, various authors have reported contrasting trends in the overall SASM variability with a few arguing for declining trend [*Fleitmann et al.*, 2003; *Sinha et al.*, 2005; *Gupta et al.*, 2005; *Kessarkar et al.*, 2010; *Saraswat et al.*, 2013; *Tiwari et al.*, 2015a] while others reporting increasing trend based on oxygen isotope ratio of planktic foraminifera [*Sarkar et al.*, 2000; *Thamban et al.*, 2001; *Tiwari et al.*, 2006; *Azharuddin et al.*, 2016] and TOC concentration of sediments [*Thamban et al.*, 1997; *Bhushan et al.*, 2001; *Tiwari et al.*, 2010] since the mid-Holocene maximum. The different trends in SASM variability can be because of the fact that the proxies used are affected by multiple factors. For example, the $\delta^{18}O$ value of foraminifera is affected by salinity, temperature, and ice-volume effect [*Tiwari et al.*, 2015b, and references therein]. Likewise, TOC concentration of sediments is influenced by preservation depending on the prevailing redox conditions and sedimentation rate [e.g., *Calvert and Pedersen*, 1993].

The TOC concentration is a widely used proxy in the Arabian Sea for reconstructing the SASM variability [*Thamban et al.*, 2001; *Kessarkar and Rao*, 2007; *Kessarkar et al.*, 2010; *Singh et al.*, 2011]. The Arabian Sea is characterized by intense phytoplankton production during summer monsoon seasons making it one of the

highest productivity zones in the world oceans [*Banse*, 1987; *Nair et al*., 1989; *Qasim*, 1997]. The majority of organic matter produced in the euphotic zone is remineralized while settling through the water column [e.g., *Berger et al*., 1989]. This process consumes dissolved oxygen while settling to the bottom [*Nair et al*., 1989]. This, accompanied by a moderate rate of thermocline ventilation by Indian Ocean Central Water, Red Sea Water, and Persian Gulf Water masses, result in massive middepth (150–1200 m) oxygen minimum zone (OMZ) in the Arabian Sea [*Wyrtki*, 1971; *Naqvi*, 1987; *Helly and Levin*, 2004]. Consequently, by far, the largest part of organic matter produced in the photic zone of the ocean (i.e., 90–99%) is ultimately recycled back to inorganic carbon [*Hedges and Keil*, 1995]. After the organic matter settles down to the bottom, benthic organisms further consume it and finally, less than 1% of the overhead surface productivity is preserved in the sediments, which is called as Sedimentary Organic Matter (SOM) [e.g., *Hedges and Keil*, 1995]. TOC concentration of the SOM in marine sediment cores is widely used as a proxy for overhead surface paleoproductivity; high/low TOC value is related to high/low paleoproductivity [*Reichart et al*., 1997; *Schulz et al*., 1998; *von Rad et al*., 1999a, 1999b]. But, preservation depending on the redox conditions and sedimentation rates along with detrital dilution in the SEAS also plays an important role in determining TOC concentration [*Sarkar et al*., 1993; *Pattan et al*., 2005; *Narayana et al*., 2009]. Thus, the possible cause for TOC increase in different regional settings is still debated.

Earlier studies from the SEAS primarily using TOC as a proxy suggested decreased productivity during the LGM [*Pattan et al*., 2003; *Avinash et al*., 2015, and references therein]. This low productivity was attributed to weaker summer monsoon wind induced upwelling. *Pattan and Pearce* [2009] have reported enhanced suboxic conditions in the SEAS over the last 140 kyr during the stadials and the glacial periods, which could have caused better preservation of TOC [*Paropkari et al*., 1991]. Additionally, studies on TOC enrichment suggests that the formation of oxygen deficient conditions, either in the oxygen minimum zone (OMZ) at intermediate water depths, or in silled basins, would have allowed better preservation and consequent enrichment of TOC in marine sediments [*Dow*, 1978; *Demaison and Moore*, 1980]. Thus, a complex interaction between overhead surface productivity, oxygen conditions, and preservation complicate the use of TOC as a productivity proxy.

In view of this, we analyzed multiple geochemical proxies viz., TOC, C/N, $\delta^{13}C_{org}$, $CaCO_3$ and major and trace elements in a sediment core from upper continental slope from the SEAS to (i) identify the sources of the SOM, (ii) determine the applicability of TOC concentration as a paleoproductivity indicator in such settings, (iii) investigate the factors responsible for TOC enrichment especially on the slope sediments that have been reported to be dominated by organic carbon maxima in this region [*Calvert et al*., 1995], and most importantly, (iv) to decipher the long-term SASM variability since mid-Holocene. This study will have major implication toward the interpretation of TOC variability in future studies from the slope sediments from the SEAS.

2. Modern Oceanographic Conditions at the Study Site

Coastal circulation in the SEAS undergoes a complete reversal associated with the two different monsoons [*Shetye and Gouveia*, 1998; *Naqvi et al*., 2006]. The West Indian Coastal Current (WICC) flows poleward during winter (northeast monsoon) causing downwelling off the western coast of India and a well-oxygenated water column over the shelf. In contrast, circulation in summer (southwest monsoon) is typical of an eastern boundary—an equatorward flowing WICC, a poleward undercurrent, and moderate coastal upwelling. What makes this region unique, apart from the seasonally reversing WICC, is that it receives enormous orographic precipitation and runoff along the southwestern coast of India in just 4 months [*Schott et al*., 2009] during the summer monsoon season. This results in the reduction of salinity as shown by the vertical profiles of salinity near the core-site (Figure 1a). Owing to the high nutrient concentrations in the freshly upwelled water (as shown by the reduction in SST by ~3°C; Figure 1c), the productivity is high [*Naqvi et al*., 2006]. During summer monsoon chlorophyll maximum (up to 7.8 μg/L) are observed in the SEAS [*Banse*, 1987]. Also, the sediment traps in the Eastern Arabian Sea have registered a doubling of the total export flux to approximately 200 mg/m^2/d [*Nair et al*., 1989] for the same season. The fairly high production is sustained till October to November [*Radhakrishna*, 1969; *Swallow*, 1984]. Consequently, the high oxygen demand for degradation of this copious organic matter leads to intense oxygen deficiency close to the surface during the summer and post-summer monsoon season (Figure

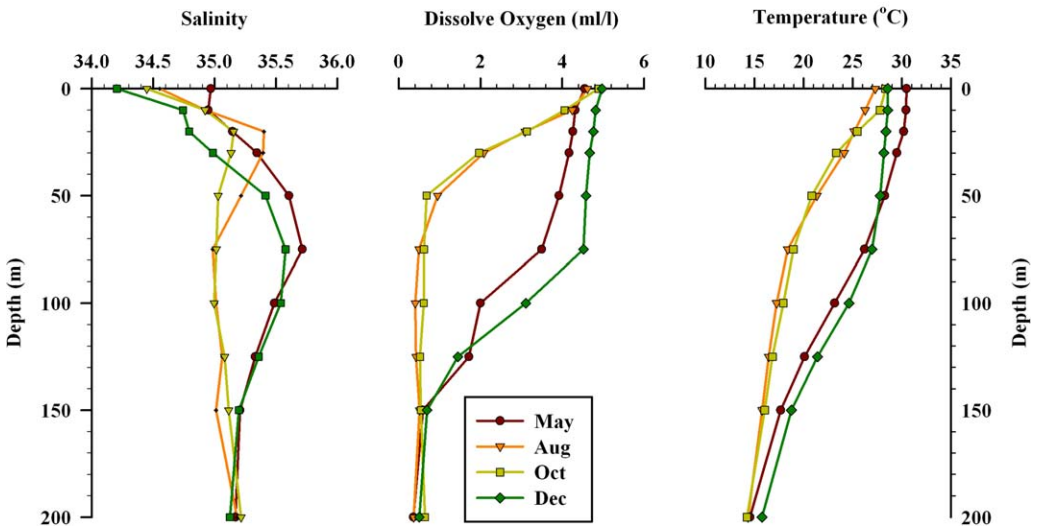

Figure 1. Modern salinity, dissolved oxygen, and temperature profiles (monthly average) near the core location. The months of August and December represent the summer and winter monsoon periods, respectively. The conditions prevailing intermonsoon periods are represented by the months of May and October. This figure is based on the World Ocean Database 2009 [*Boyer et al*., 2009].

1b). An intense OMZ from ~150 to 1200 m exists year-round supported by high productivity, advection of water masses with a high amount of organic matter from the western Arabian Sea, and flow of intermediate water masses with low oxygen content.

3. Materials and Methods

3.1. Chronology

A 36 cm long gravity core named SN-6 was retrieved from the upper continental slope of the SEAS (12°29′021″N: 74°07′966″E; water depth 589 m) during the return-leg of the 4th Indian Southern Ocean Expedition (Figure 2). The core was subsampled at 1 cm interval. The Accelerator Mass Spectrometer (AMS) ^{14}C chronology of the core was obtained from the National Science Foundation-AMS Laboratory, University of Arizona, USA. The details of the chronology have been reported in *Tiwari et al*. [2015a]. The Age-depth model (Figure 2) shows that the core-top (0–1 cm) is dated at 154 ± 44 yr BP (1σ) while the last dated section (35–36) age is 4772 yr BP. The sedimentation rates observed for the top 11 cm in the present study is 16.2 cm/kyr (i.e., a resolution of ~62 years/cm) while the average resolution is 127 years/cm yielding, thus, a centennial scale resolution.

3.2. Elemental Analysis of Total Organic Carbon and Total Nitrogen

For %TOC and %TN analysis, each subsample was oven dried at 40°C and then homogenized by finely grounding it in an agate mortar. For %TOC, carbonate was removed from the subsample by adding 2N hydrochloric acid. The samples were then completely rinsed by adding deionized water for around five times and again oven dried at 40°C. In the case of %TN analysis, untreated samples were used. A portion of the ground sample was then wrapped in a tin capsule and combusted using an Elemental Analyzer at the Marine Stable Isotope Lab (MASTIL) at National Centre for Antarctic and Ocean Research (NCAOR), Goa, India. The analytical precision based on repeated measurements (n = 18) of the reference standard Sulphanilamide for %TOC and %TN measurements is ±0.2% and ±0.3%, respectively. The $CaCO_3$ content of the sediment was calculated by first calculating the inorganic carbon by subtracting the TOC from the Total Carbon and then multiplying by 8.33 to convert to $CaCO_3$ content [$CaCO_3$ (%) = (Total Carbon − TOC) × 8.33]. The analytical precision based on standard error propagation techniques is ±0.3% for the $CaCO_3$ content. The Mass Accumulation Rate (MAR) of various geochemical proxies ($CaCO_3$, TOC) has been calculated by multiplying concentration by dry bulk density (DBD) and sedimentation rate. The DBD has been calculated using the empirical equation derived by *Clemens et al*. [1987].

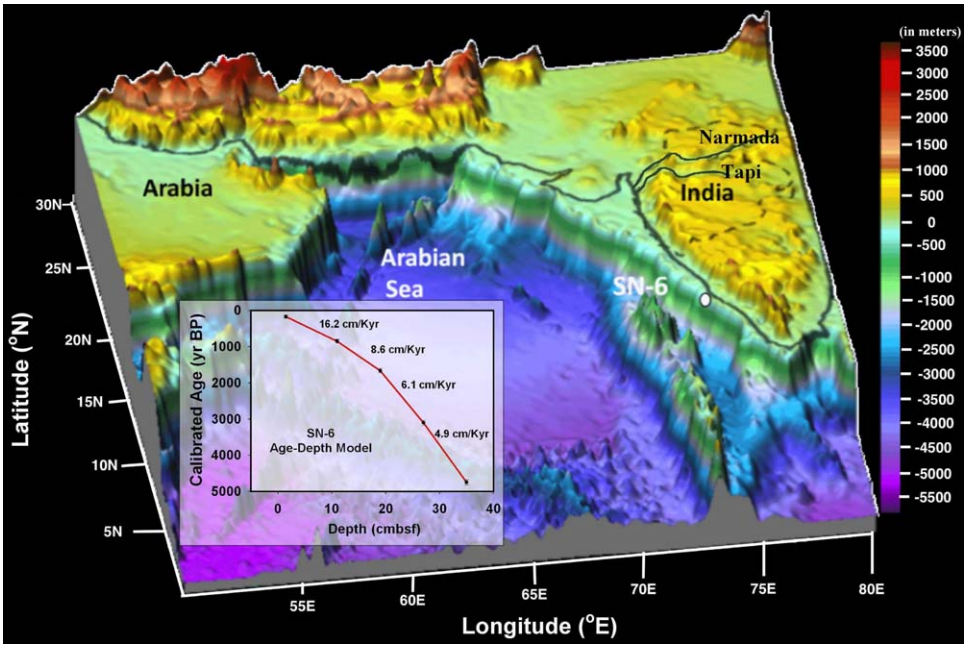

Figure 2. Location of the core (shown by the closed circle) and the bathymetry of the study area. Core SN-6 is from the upper continental slope of India. The inset shows the age-depth model based on five radiocarbon dates approximately at every 9 cm on selected species of planktic foraminifera; sedimentation rates are also shown (in cm/kyr).

3.3. Carbon Stable Isotope Ratios

For the analysis of stable isotope of carbon ($\delta^{13}C_{org}$), carbonate-free samples were used. $\delta^{13}C_{org}$ values were determined using an Isoprime stable isotope ratio mass spectrometer after high-temperature flash combustion in an elemental analyzer at 950°C. Samples were run with blank and known standards. Standards were prepared by weighing 0.4–0.6 mg of IAEA cellulose standard (IAEA-CH-3) of certified isotopic composition ($\delta^{13}C = -24.74‰$ versus VPDB). Data quality control was checked by running reference standard after every six samples. Stable isotope values were reported in per mil (‰) while the delta notation is defined as $\delta^{13}C$ (‰) = $[(R_{Sample} - R_{Standard})/R_{Standard}] \times 1000‰$; where R_{sample} and $R_{reference}$ are the isotopic ratios ($^{13}C/^{12}C$) of sample and reference, respectively. Analytical precision based on repeated measurements of the reference standard (n = 18) was better than 0.02‰.

3.4. Inorganic Elemental Analysis

For inorganic elemental chemistry, sediments were dissolved following acid digestion procedure by *Balaram and Rao* [2003]. The powdered sediment samples (n = 36) were weighed accurately (50 mg), transferred to clean Teflon beakers and subjected to open acid digestion. The sediments were repeatedly digested by treating with a mixture of HF, HNO_3, and $HClO_4$ in the ratio of 6:3:1. Finally, the extract was brought to a standard volume (50 ml). All elements were analyzed using inductively coupled plasma mass spectrometry at National Centre for Antarctic and Ocean Research, Goa. Analytical accuracy was determined through analysis of a suite of internationally recognized Standard Reference Material (NIST 2702). The relative standard deviation estimates based on repeated analysis of standards for all elements discussed here are better than ±10%.

4. Results and Discussion

4.1. Enhanced Reducing Conditions in the SEAS Since Mid-Holocene

We studied a suite of inorganic metals (Al, Ti, Fe, Mn, Cr, V, Mo, Cu, Zn, Ni, and Co) to investigate the role of past geochemical changes on the preservation of organic matter [e.g., *Morford and Emerson*, 1999]. The abundances of most of these elements are controlled by (1) terrigenous fraction (fluvial and aeolian), (2) biogenic fraction—related to carbonates and organic matter, and (3) authigenic fraction—composed of insoluble oxyhydroxides and sulfides [*Riquier et al*., 2006]. Aluminum is commonly used as a proxy for land-

Table 1. Regression Coefficients (r^2) of Al and $CaCO_3$ With Selected Major and Trace Elements and Level of Significance of Correlation (p) for 36 Samples

	Al		$CaCO_3$	
Elements	r^2	p	r^2	p
Ti	0.96	<0.0001	0.09	0.0721
Fe	0.98	<0.0001	0.11	0.0431
Mn	0.80	<0.0001	0.23	0.0034
Cr	0.91	<0.0001	0.29	0.0007
V	0.34	0.0002	0.41	<0.0001
Mo	0.23	0.0028	0.03	0.3327
Cu	0.00	0.9139	0.08	0.1024
Zn	0.00	0.8528	0.23	0.003
Ni	0.39	<0.0001	0.49	<0.0001
Co	0.70	<0.0001	0.09	0.0653
$CaCO_3$	0.15	0.0202	N.A	N.A

derived aluminosilicate fraction of the sediments with very little affinity to move during diagenesis [*Brumsack*, 1989; *Calvert and Pedersen*, 1993] and calcium carbonate is primarily considered as the biogenic product of marine origin. So, in order to identify the origin (detrital, biogenic, or authigenic) of the studied elements in our core, correlation of aluminum and calcium carbonate with selected elements was determined using linear regression (least square method) for 36 samples using the statistical package—SigmaPlot 12.0. A high regression coefficient (r^2) value of these metals with Al indicates the detrital source (supporting information Figure 1) and with that of $CaCO_3$ indicates the biogenic source (supporting information Figure 2) [e.g., *Acharya et al*., 2015]. The regression coefficient values (Table 1) indicate that elements such as Ti, Fe Mn, Cr, and Co have a siliciclastic origin and their fluctuations in sediments can be explained in terms of the variation in the detrital influx. V and Ni show moderate regression coefficient values with Al and $CaCO_3$. While elements such as Mo, Cu, and Zn show very poor correlation with Al and $CaCO_3$ thereby suggesting an authigenic source.

In addition to the element/Al ratio, enrichment factors of selected trace metals (Table 2) have been evaluated to determine the redox conditions during the sediment deposition. The enrichment factor (EF) for an element X has been determined by the formula $EFX = (X/Al)_{sample}/(X/Al)_{average\ shale}$, where the average shale values were taken from *Wedepohl* [1971]. Thus, the enrichment factor of redox-sensitive may, therefore, indicate anoxic/oxic conditions at the seafloor or within the sediment. Elements with siliciclastic origin show some enrichment with regard to its shale values thereby suggesting reducing environment during the time of deposition since mid-Holocene. Maximum enrichment shown by Mo, Cu, and Zn can be due to its authigenic source of origin as they show very poor correlation with Al and $CaCO_3$. Therefore, to estimate the fraction of elements that are not derived from the terrigenous input, the authigenic fraction was estimated for a trace metal X by the standard formula; Authigenic X = Total X − (Al sample × (X/Al) reference material). Average shale [*Wedepohl*, 1971] and Al are generally used as reference component to calculate the authigenic fraction of metals [*Calvert and Pedersen*, 1993; *Morford and Emerson*, 1999; *Tribovillard et al*., 2006]. We used the ratio R= (Cu + Mo/Zn) proposed by *Hallberg* [1976], as an indicator of the oxygenation of bottom waters. The basic principle behind the use of this ratio lies in the fact that in reduced environment with H_2S in bottom water, the precipitation of Cu is favored over Zn in the sediments, which is the result of differences in the solubility product of their sulfides in reduced environments [*Hallberg*, 1976]. Hence, this ratio is expected to increase under suboxic conditions and decrease under oxidizing conditions. The variation of R from a minimum value of 0.14 during mid-Holocene to the maximum value of 2.01 toward present reflects the increasing reducing conditions since mid-Holocene.

Table 2. Average Redox-Sensitive Element/Al Ratio for SN-6 Sediments and Average Shale [*Wedepohl*, 1971][a]

	Element/Al Ratio (ppm/%)				Enrichment Factor
	Core SN-6				
Trace Elements	Max	Min	Average	Average Shale	
Cr	16.49	13.80	15.24	10.2	1.45
V	42.49	11.81	24.51	15	1.65
Mo	1.44	0.71	1.11	0.15	7.73
Cu	27.86	14.89	19.87	5.1	4.21
Zn	109.37	16.77	44.64	11	4.58
Ni	12.31	0.46	4.1	7.7	0.43
Co	3.61	2.63	3.11	2.1	1.48

[a]The enrichment factors (EF) for various elements in studied samples are calculated wrt average shale.

We further examined the interelemental relationships of redox-sensitive trace elements, as they become moderately to highly enriched under suboxic bottom water conditions, making them useful as indicators of paleo-redox conditions. In marine sediments, Mo is considered as a proxy of redox conditions because of its conservative behavior in oxygenated waters and enrichment in anoxic sediments. In oxic environments, Nickel behaves as a micronutrient, which occurs as soluble Ni^{2+} or $NiCl^{+}$ ion [*Tribovillard et al*., 2006]. Nickel complexation with

organic matter accelerates scavenging in the water column and thus its enrichment in sediments [*Calvert and Pedersen*, 1993]. Unlike Ni, Cobalt behaves similarly as Mn in seawater and sediments, i.e., it can diffuse out of sediments under reducing conditions [*Heggie and Lewis*, 1984] and hence increase the Ni/Co ratio. The V/Cr ratio is a redox indicator, which reflects changes in the scavenging efficiency as a function of redox conditions [*Jones and Manning*, 1994; *Riquier et al*., 2006; *Gallego-Torres et al*., 2010]. Under oxic conditions, vandate adsorbs more strongly than chromate, whereas in reducing condition Cr (III) forms stronger surface complexes than VO^{2+}. Unlike V which starts precipitating in suboxic condition, Mo only starts to precipitate when dissolved sulfide (H_2S) is available (euxinic condition). In the present study, Ni/Co, V/Cr, and V/Mo ratio ranges from 0.01 to 3.75, 0.85 to 2.75, and 8.43 to 37.12, respectively. All the three ratios show an increase in reducing conditions from 4772 to 3955 yr BP followed by a slight decline thereafter. Another episode of increase in reducing conditions is seen from 3342 to 2795 yr BP that is again followed by a decline in reducing conditions with the major decline seen at 1813 yr BP. After this period, we see an increase in reducing conditions till 278 yr BP with a slight decline in reducing periods observed between 1326–1093 and 710–525 yr BP. From 278 yr BP to present, we again see a slight decline in reducing conditions. Although, we see some declining periods of reducing conditions, the long-term trend shown by these redox proxies (Figures 3f, 3g, and 3h) shows an increase in reducing conditions resulting in intensified OMZ conditions since mid-Holocene. Further, the persistent low Mn/Al ratio (mean = 14.47 ppm/%), which is about a factor of 10 lower than that in shale value (106 ppm/% for Mn/Al) [*Wedepohl*, 1971] suggests that the bottom water remained suboxic at the studied location throughout the period of deposition. Mn/Al ratios in detrital materials of the river Narmada and Tapi, which drain into this region, are still higher, 147 ± 20 ppm/%. *Agnihotri et al*. [2003a] based on low Mn/Al ratio since mid-Holocene to present in the core 3268G5 (water depth 600 m, 12.5°N, 74.2°E) near Mangalore offshore, also suggests that the bottom water remained suboxic at the studied location throughout the period of deposition. *Naik et al*. [2014] by using the enrichment of Mo and Cr reported the prevalence of suboxic depositional environment from late Holocene to present in the sediments from Goa offshore (Core AAS9/19; water depth of 367 m, 14°30.115′N; 73°08.515′E), which was also observed by *Agnihotri et al*. [2003a] as evidenced by increasingly higher $\delta^{15}N$ values. Recently, *Saraswat et al*. [2016] based on the relative abundance of the angular asymmetrical benthic foraminifera—an indicator of bottom water oxygenation—showed a declining dissolved oxygen concentration since mid-Holocene.

4.2. TOC and $CaCO_3$ Concentration: Implications to SASM Variability Since Mid-Holocene

The accumulation of calcium carbonate on the seafloor is mainly controlled by the surface water biological production, rate of dissolution during its journey through the water column as well as on the seafloor and dilution by the noncarbonate fraction and terrigenous matter. The regional lysocline depth in the study region is at 3800 m [*Peterson and Prell*, 1985] and the present sediment core was retrieved from 590 m water depth suggesting that dissolution of calcium carbonate is negligible in the SEAS. The % $CaCO_3$ in the present study varies from 18.79% to 1.23%. $CaCO_3$ mass accumulation rate does not show any trend (Figure 3b) whereas the long-term trend shown by $CaCO_3$ concentration in the present study shows a decline since mid-Holocene (Figure 3c) with the increasing sedimentation rate suggesting that terrigenous dilution could be cause for its variation. But, the terrigenous dilution as a possible cause for $CaCO_3$ variations is excluded based on the fact that the positive correlation between both variables is weak ($r^2 = 0.15$). The inverse relationship observed between the overall trend of $CaCO_3$ (%) and TOC (%) ($r^2 = 0.57$, $p \leq 0.0001$, see supporting information Figure 4) can be due to the enhanced availability of CO_2 in the OMZ. Accumulation of remineralization end products in OMZs result in a Dissolved Inorganic Carbon (DIC) maxima, which is known as Carbon Maximum Zones (CMZ) [*Paulmier et al*., 2011]. They can act as a local source of CO_2 [*Paulmier et al*., 2011] and can dissolve $CaCO_3$ on the seafloor [*Naik et al*., 2014]. Therefore, we propose that the observed decline in $CaCO_3$ concentration in the present study is due to the dissolution of $CaCO_3$ as a result of enhanced reducing conditions (low oxygen concentration, strengthened OMZ, and CMZ) since mid-Holocene. This is further supported by another study from a nearby core (AAS9/19) that observed a similar decline in $CaCO_3$ (%), which was attributed to the dissolution effect as a result of strengthened reducing conditions since mid-Holocene [*Naik et al*., 2014].

Sedimentary TOC as a proxy of in-situ productivity related to the SASM intensity in coastal sediments of the SEAS possess an inherent limitation that whether they are of marine (in-situ produced) or terrestrial (transported via numerous streams/surface runoff) origin [*Muller and Suess*, 1979]. Traditionally, source

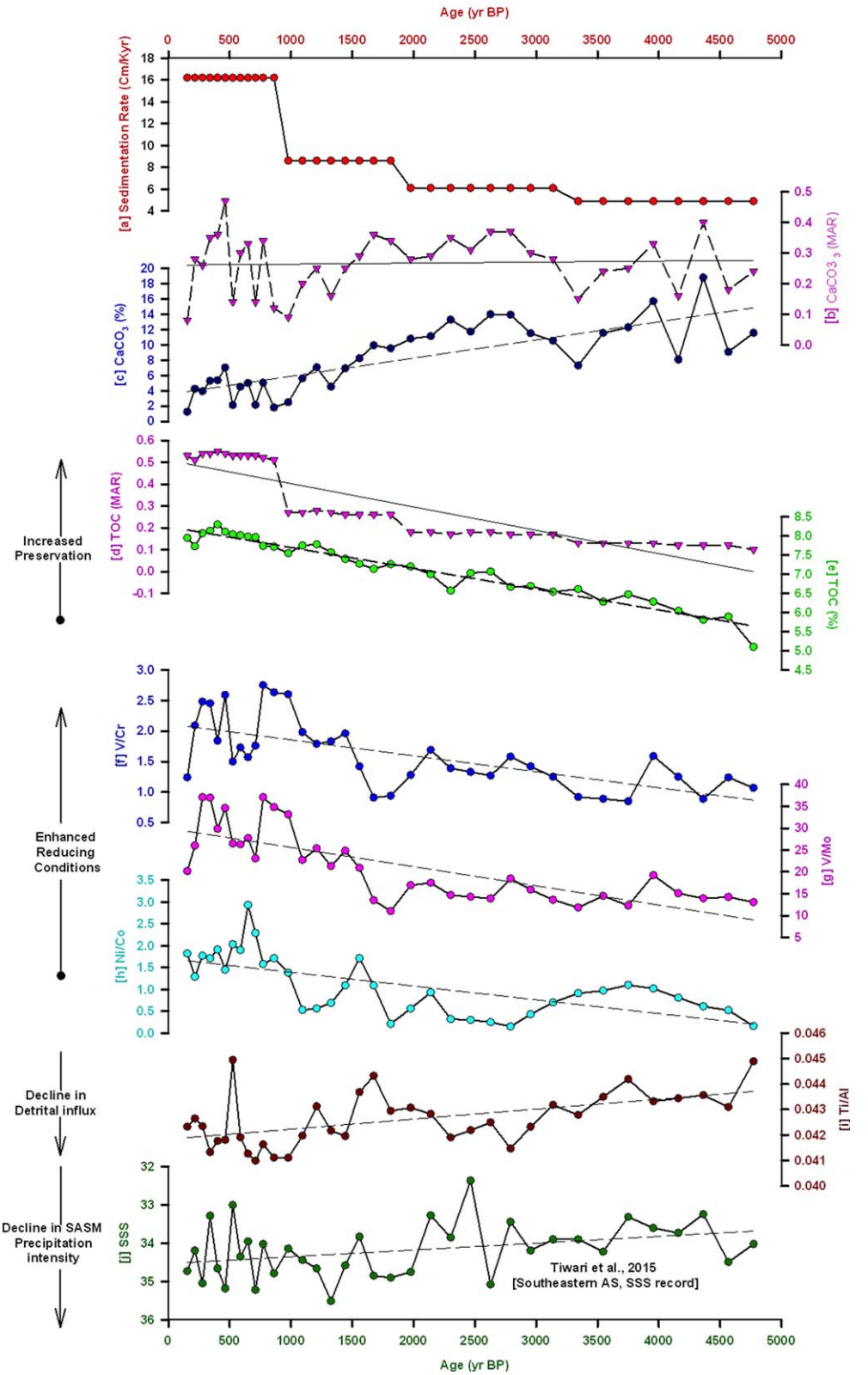

Figure 3. Downcore variation of geochemical proxies: (a) sedimentation rate; (b) $CaCO_3$ mass accumulation rate; (c) $\%CaCO_3$; (d) total organic carbon mass accumulation rate; (e) %total organic carbon as a function of preservation; (f)–(h) V/Cr, V/Mo, and Ni/Co indicating redox condition; (i) Ti/Al indicating decline in detrital influx since mid-Holocene; and (j) sea surface salinity showing SASM precipitation strength.

characterization of organic matter is done using carbon isotopes ($\delta^{13}C_{org}$) and atomic C/N wt. ratio. *Fontugne and Duplessy* [1986] reported typical $\delta^{13}C_{org}$ of terrestrial and marine organic matter of the Arabian Sea as $-26‰$ and $-20‰$, respectively (with respect to PDB). Likewise, mean C/N wt. ratio ranges $\sim 8.0 \pm 2$ for a typical marine organic matter in this region [*Calvert et al*., 1995; *Bhushan et al*., 2001]. Despite heavy monsoonal precipitation runoff on the west coast of India, several studies reported majority of the organic matter is typically "marine" even in very shallow environment [*Bhushan et al*., 2001; *Agnihotri et al*., 2002, 2003a]. In the present study, the $\delta^{13}C_{org}$ values vary between $-22.35‰$ and $-21.17‰$, with an average of $-21.56‰$. Whereas atomic C/N ratios show higher values ranging between 18.21 and 23.22 with an average of 20.38 revealing marine as well as terrestrial sources of organic matter. The plot of $\delta^{13}C_{org}$ versus atomic C/N (supporting information Figure 3) shows a signal of mixed sources: marine organic matter, as well as significant amount of terrestrial organic matter, is present. It suggests that the traditional paleoproductivity proxy, i.e., TOC concentration, cannot be ascribed solely to the surface water productivity in such settings. The timing and the magnitude of change in the TOC concentration are attributed to regional oceanographic features, mainly productivity, surface current direction, terrigenous input, and dissolved oxygen that affect both the flux of autochthonous and allochthonous material, and its deposition and diagenetic alteration. The long-term declining trend shown by Ti/Al (Figure 3i) in the present study suggests a decline in surface runoff/detrital influx resulting in a decline in terrestrial organic carbon input. So, enhanced runoff bringing more terrestrial organic matter is ruled out. The lack of an independent surface water productivity indicator in the present study does not allow us to examine the relative contribution of marine organic carbon. However, the previous study from the same region based on changes in relative abundance of planktic foraminifera *Globigerina bulloides* (an indicator of high productivity) suggests a decline in marine productivity since mid-Holocene [*Saraswat et al*., 2016]. Therefore, the increasing trend observed in the TOC mass accumulation rate and concentration (Figures 3d and 3e) since mid-Holocene to present can be interpreted either in terms of the sedimentation rate variation and/or changes in redox conditions in bottom waters/sediment-water interface. Both these factors can play a major role in the preservation of TOC, resulting in its deviation from the surface productivity trend. However, as discussed above in section 2, the periods of slight decline in reducing condition are not coeval with the enhanced TOC values observed in the present study since mid-Holocene to present. *Canfield* [1994] observed that the sediment deposition rate is overall the most important factor influencing TOC preservation, as it provides less time for organic matter to degrade. *Canfield* [1994] also proposed a similar preservation of TOC irrespective of presence or absence of bottom water O_2, at sedimentation rates higher than $\sim$40 cm/kyr in normal marine conditions. In the case of marine sediments depositing with sedimentation rates below 40 cm/kyr, enhanced preservation of TOC may be found under low bottom-water O_2 conditions. In the studied core, the high sedimentation rate of 16.2 cm/kyr is observed for the top 11 cm with the average sedimentation rate of 8.96 cm/kyr (Figure 3a), which is much lower than 40 cm/kyr. *Somayajulu et al*. [1999] and *Agnihotri et al*. [2003b] also observed similar sediment accumulation rates ($\sim$20 cm/kyr) at 370, 600, and 1680 m water depths on the continental slope off Mangalore. Sediment cores lying outside the OMZ of the eastern Arabian Sea were found to have a much lower abundance of TOC contents due to much lower sedimentation rates and thereby longer exposure time to oxic waters at the sediment-water interface leading to a poor preservation [*Agnihotri et al*., 2003a]. Therefore, the increased sedimentation rate observed in the present study along with the enhanced bottom-water reducing conditions must have caused limited organic matter decomposition within the water column, resulting in enhanced TOC values in the SEAS and its deviation from the surface productivity trend. This is further corroborated by a strong correlation between TOC and TN ($r^2 = 0.88$) (supporting information Figure 4).

The qualitative changes in past SASM have been reconstructed from both the SEAS [*Schulz et al*., 1998; *von Rad et al*., 1999a, 1999b; *Lückge et al*., 2001; *Altabet et al*., 2002; *Agnihotri et al*., 2002; *Anderson et al*., 2002] and from the Indian subcontinent [*Ramesh et al*., 1985; *Sinha et al*., 2005; *Yadav*, 2013] at centennial to subcentennial scale resolution. However, the quantitative estimates of SASM intensity (based on $\delta^{18}O$ of foraminifera, Mg/Ca, a proxy for seawater temperature) are limited and have coarse resolution [*Saraswat et al*., 2005; *Anand et al*., 2008; *Banakar et al*., 2010; *Govil and Naidu*, 2011; *Saraswat et al*., 2012]. Recently, past salinity values determined from the same core used in the present study at a high-resolution of centennial scale has shown declining SASM precipitation intensity since mid-Holocene [*Tiwari et al*., 2015a] (Figure 3j). This is further accompanied by the declining long-term trend shown by Ti/Al (Figure 3i) in the present study, which suggests a decline in surface runoff/detrital influx with the declining SASM precipitation

intensity. The sedimentation rate in the present study has shown a gradual increase from 4772 to 977 yr BP, whereas the drastic change in the sedimentation rate is observed only after 1000 yr BP to present thereby showing an increasing long-term trend. However, the observed long-term trend shown by the sedimentation rates in the present study do not match with declining SASM intensity since mid-Holocene. But if we look at the short-term changes in Ti/Al, it shows an increase during the time of increased sedimentation rate, i.e., from 3342 to 3137 yr BP, from 1976 to 1813 yr BP, and from 977 yr BP to present thereby suggesting an increase in terrigenous influx with increasing sedimentation rate. Interestingly, this time intervals are further accompanied by a decrease in SSS suggesting an increase in SASM intensity. Thus, the nonconsistent long-term trend of sedimentation rate observed in the present study is could be due to fewer numbers of dates and the same could be improved by dating few more number of samples in between to get a clear picture. Therefore, we note that, although there were few periods of enhanced SASM intensity, the long-term trend shown by surface run-off/detrital influx suggests decline in the SASM intensity since mid-Holocene, which corroborates the previously determined decline in SASM precipitation [*Kessarkar et al*., 2013; *Saraswat et al*., 2013; *Tiwari et al*., 2015a].

4.3. Response of Monsoon System to Precessional Forcing Since Mid-Holocene: Comparison Between South Asian, East Asian, and North African Summer Monsoon

The Indian monsoon represents the most typical monsoon climate, as it is characterized by (i) a robust annual reversal of the prevailing surface winds (summer south-westerlies and winter north-easterlies) and (ii) a sharp contrast between rainy summer and arid winter, with 70–80% of the total annual precipitation falling in June-July-August-September [*Webster*, 1987]. In general, it seems that the SASM precipitation since mid-Holocene transits between dry and wet conditions [e.g., *Yadava and Ramesh*, 2005; *Laskar et al*., 2013; *Prasad et al*., 2014; *Tiwari et al*., 2015a] but the overall trend since mid-Holocene is still debatable. The spectral analysis and numerical modeling indicate that the low-latitude climate and SASM variability are mainly caused by changes in precession [*Molfino and McIntyre*, 1990; *Clemens et al*., 1991; *McIntyre and Molfino*, 1996; *Joussaume et al*., 1999; *Jiang et al*., 2013]. The precessional cycle does not change insolation's annual total, but rather influences its seasonality and in turn that of the monsoon, significantly. Since seasonal variations are out of phase between hemispheres, the insolation changes associated with precession are also out of phase, resulting in hemispheric contrasts in paleomonsoon records at the precessional timescale. The precession forcing of the monsoon is most evident in proxy records since mid-Holocene, given the richness of geological data archives and particularly the high-resolution terrestrial and marine records from the Indian, African, and East Asian monsoon regions. For example, a few of the SASM wind intensity, based proxies such as the relative abundance of *G. bulloides* from the ODP site 723-A from the western Arabian Sea [*Gupta et al*., 2005] (Figure 4d) showed that the SASM has declined since mid-Holocene with the declining NH solar insolation. Recent study by *Tiwari et al*. [2015a], based on paired measurement of stable oxygen isotopic ratio and trace metal composition of surface dwelling planktic foraminifera for the same core SN-6, helps in estimating past salinity which is mainly controlled by local evaporation-precipitation, thus providing a good idea of monsoon intensity. Increasing values of SSS since mid-Holocene to present corresponds to weakened SASM conditions leading to arid climate (Figure 4b). A similar decline in SSS in the SEAS is also shown by *Kessarkar et al*. [2013] suggesting declining SASM intensity since mid-Holocene. Sea surface salinity and $\delta^{18}O_{seawater}$ are directly linked to the local E-P balance, and in general, a good linear correlation can be found between these parameters for most of the global ocean [*Craig and Gordon*, 1965]. Thus, by studying the $\delta^{18}O_{seawater}$, *Saraswat et al*. [2013] show the evidence of high saline surface water since mid-Holocene indicating a decline in freshwater runoff from the Western Ghats as a consequence of declining SASM intensity since mid-Holocene. Also, the terrestrial records from Qunf Cave, southern Oman [*Fleitmann et al*., 2003] (Figure 4c), Timta Cave, northern India [*Sinha et al*., 2005], and Tianmen Cave, Tibet [*Cai et al*., 2012] suggest that the Indian monsoon has varied in concert with the declining Northern Hemisphere solar insolation after attaining maxima during mid-Holocene. Furthermore, stalagmites from East Asia exhibit a long-term trend that is broadly similar to changes in Northern Hemisphere solar insolation, with a general warm/wet period in NH monsoon regions at 5.0 ka BP, which corresponds to the Holocene climatic optimum followed by cold/arid period since then (Figures 4f and 4g). A similar pattern has also been observed in marine and terrestrial proxy records of the North African monsoon. Africa is presently the only continent that is divided by the Equator into two nearly equal parts, resulting in distinct monsoon systems in each hemisphere. Rich geological archives of the North African monsoon have been recovered from the East African Rift lakes [*Gasse et al*., 2008], the Mediterranean Sea [*Ziegler et al*., 2010], the North

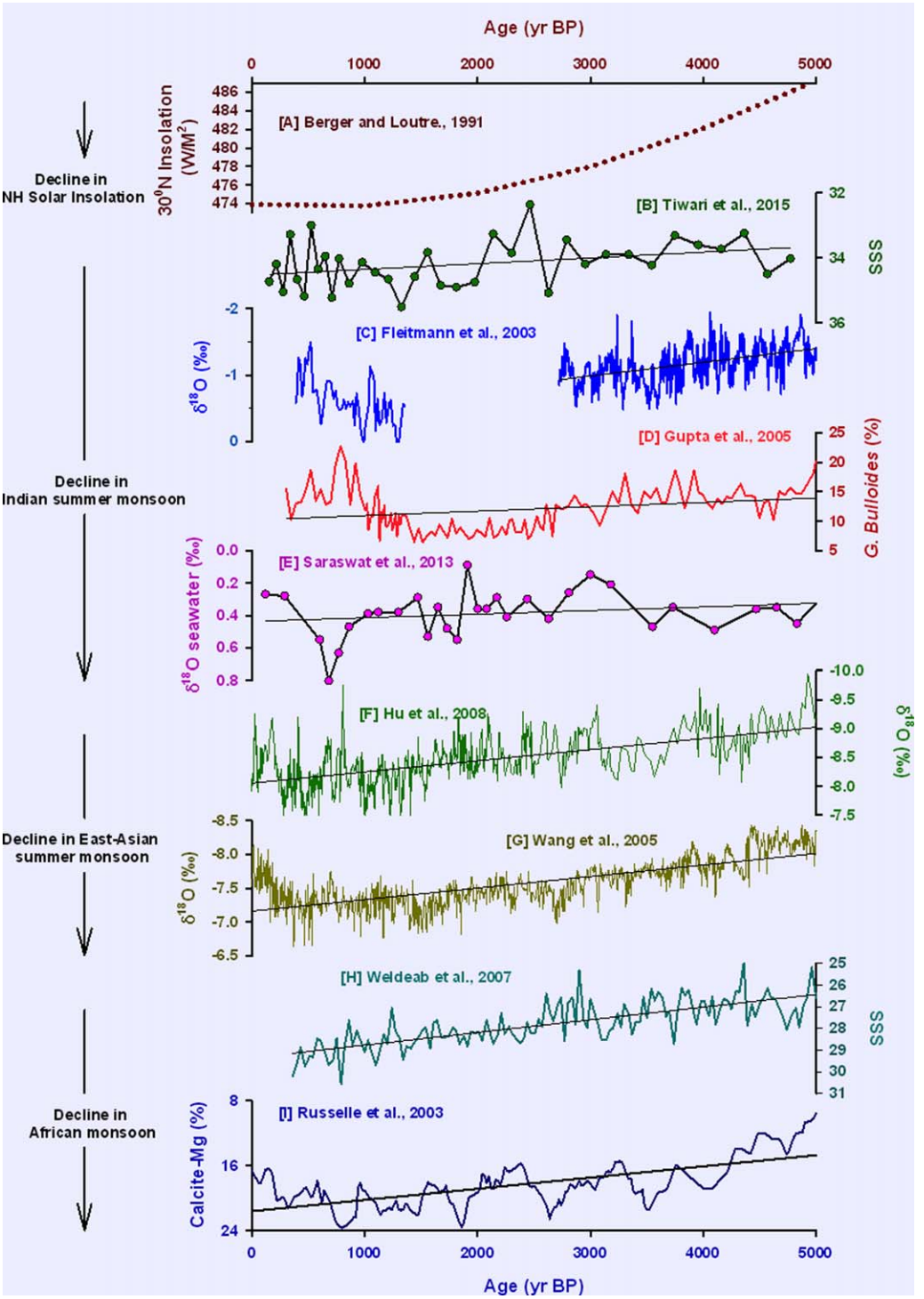

Figure 4. Comparing records of (b–e) Indian summer, (f and g) East Asian summer monsoons, and (h and i) African summer monsoon using diverse proxies from different regions and its response to precessional forcing. Figure 4a shows June insolation at 30°N.

Atlantic [*Pokras and Mix*, 1987; *Weldeab et al*., 2007], as well as caves [*Bar-Matthews et al*., 2003]. As a result, the history of the North African monsoon is better resolved by proxy data than its southern counterpart. The precipitation record from the marine sediment core in the Gulf of Guinea (MD03–270), an indicator of relative changes in the outflow of the Niger and Sanaga rivers shows a decline since 5 ka BP [*Weldeab et al*., 2007] (Figure 4h). Likewise, Mg percentage in calcite from Lake Edward, an equatorial rift lake in central

Africa, is used to reconstruct lacustrine paleohydrology and climate history. The Mg percentage in calcite rises during evaporative concentration of a lake because of increases in the $[Mg^{2+}]/[Ca^{2+}]$ ratio in lake water. The observed decline in Mg percentage in calcite suggest increased aridity since mid-Holocene [*Russell et al*., 2003] (Figure 4i). Thus our intercomparison study suggests that basic structures of variability for the Indian, East Asian, and African monsoons are remarkably similar. It exhibits a long-term trend broadly tracking the intensity of northern hemisphere summer insolation [*Yuan et al*., 2004; *Wang et al*., 2008; *Cheng et al*., 2009; *Zhang et al*., 2011; *Cai et al*., 2012] suggesting a decline in seasonal heating resulting in colder summer in the Northern Hemisphere since mid-Holocene. It is likely therefore that the NH summer monsoons are not only governed by a common set of processes, such as the enhanced east-west thermal contrast in the Indo-Pacific, but also by interhemispheric thermal asymmetries associated with their contrasting land extents that have potentially opposing effects on the NH and SH monsoons [*Wang et al*., 2012].

5. Conclusions

A suite of geochemical proxies, including major and trace elements, have been used to reconstruct past redox conditions and SASM variability from SEAS since mid-Holocene. Various redox proxies (viz. enrichment and interelemental relationships of redox-sensitive trace elements) indicate intensified reducing conditions there by suggesting the strengthening of the OMZ since mid-Holocene to the present. Atomic C/N ratio versus the $\delta^{13}C_{org}$ plot shows that the core site has experienced mixed productivity signal since mid-Holocene thereby limiting the use of TOC as a productivity indicator in such settings. We find that the enhanced TOC values observed in the present study are a result of better preservation caused by increased sedimentation rate under the prevalence of enhanced suboxic bottom waters suggesting intensified OMZ since mid-Holocene. Past SASM variability as shown by Ti/Al in the present study indicates a decline since mid-Holocene, which matches with the previous studies. Thus, this study would help to understand past SASM variability more accurately in future studies from this region. The intercomparison of monsoon records from different regions shows declining monsoon since mid-Holocene implying the influence of the precessional forcing. It suggests an increased/reduced seasonal heating during the northern/southern hemisphere summer during the mid-Holocene resulting in stronger/weaker summer monsoon in the northern/southern hemisphere and vice versa in winter. More of such studies involving quantitative estimates coupled with model ensemble are required to assess the role played by various forcing factors.

Acknowledgments
We thank the Ministry of Earth Sciences and National Centre for Antarctic & Ocean Research (NCAOR) for support and encouragement (NCAOR contribution 24/2017). We also thank ISRO-GBP for support. Thanks are due to Dr. Thamban Meloth and Mr. Prashant Redkar of NCAOR for help in the analysis of major and trace elements on ICP-MS. The data for this paper can be accessed through the supporting information or by direct request to the corresponding author.

References

Acharya, S. S., M. K. Panigrahi, A. K. Gupta, and S. Tripathy (2015), Response of trace metal redox proxies in continental shelf environment: The Eastern Arabian Sea scenario, *Cont. Shelf Res.*, *106*, 70–84.

Agnihotri, R., K. Dutta, R. Bhushan, and B. L. K. Somayajulu (2002), Evidence for solar forcing on the Indian monsoon during the last millennium, *Earth Planet. Sci. Lett.*, *198*, 521–527.

Agnihotri, R., S. K. Bhattacharya, M. M. Sarin, and B. L. K. Somayajulu (2003a), Changes in surface productivity and subsurface denitrification during the Holocene: A multiproxy study from the eastern Arabian Sea, *Holocene*, *13*, 701–713, doi:10.1191/0959683603hl656rp.

Agnihotri, R., M. M. Sarin, B. L. K. Somayayajulu, A. J. T. Jull, and G. S. Burr (2003b), Late-Quaternary biogenic productivity and organic carbon deposition in the Eastern Arabian Sea, *Palaeogeogr. Palaeoclimatol. Palaeoecol.*, *197*, 43–60.

Altabet, M. A., M. J. Higginson, and D. W. Murray (2002), The effect of millennial-scale changes in Arabian Sea denitrification on atmospheric CO_2, *Nature*, *415*, 159–162.

Anand, P., D. Kroon, A. D. Singh, R. S. Ganeshram, G. Ganssen, and H. Elderfield (2008), Coupled sea surface temperature seawater $\delta^{18}O$ reconstructions in the Arabian Sea at the millennial scale for the last 35 ka, *Paleoceanography*, *23*, 4207, doi:10.1029/2007PA001564.

Anderson, D. M., J. T. Overpeck, and A. K. Gupta (2002), Increase in the Asian SW Monsoon during the past four centuries, *Science*, *297*, 596–599.

Avinash, K., B. R. Manjunath, and P. J. Kurian (2015), Glacial-interglacial productivity contrasts along the eastern Arabian Sea: Dominance of convective mixing over upwelling, *Geosci. Frontiers*, *6*, 913–925.

Azharuddin, S., P. Govil, A. D. Singh, R. Mishra, S. Agrawal, A. K. Tiwari, and K. Kumar (2016), Monsoon-influenced variations in productivity and lithogenic flux along offshore Saurashtra, NE Arabian Sea during the Holocene and Younger Dryas: A multi-proxy approach, *Palaeogeogr. Palaeoclimatol. Palaeoecol.*, *483*, 136–146, doi:10.1016/j.palaeo.2016.11.018.

Balaram, V., and T. G. Rao (2003), Rapid determination of REEs and other trace elements in geological samples by microwave acid digestion and ICP-MS, *At. Spectrosc.*, *24*, 206–212.

Banakar, V. K., B. S. Mahesh, G. Burr, and A. R. Chodankar (2010), Climatology of the Eastern Arabian Sea during the last glacial cycle reconstructed from paired measurement of foraminiferal $\delta^{18}O$ and Mg/Ca, *Quat. Res.*, *73*, 535–540.

Banse, K. (1987), Seasonality of phytoplankton chlorophyll in the central and northern Arabian Sea, *Deep Sea Res., Part A*, *34*, 713–723.

Bar-Matthews, M., A. Ayalon, M. Gilmour, A. Matthews, and C. J. Hawkesworth (2003), Sea-land oxygen isotopic relationships from planktonic foraminifera and speleothems in the Eastern Mediterranean region and their implication for paleorainfall during interglacial intervals, *Geochim. Cosmochim. Acta*, *67*, 3181–3199.

Berger, W. H., V. S. Smetacek, and G. Wefer (1989), Ocean productivity and paleoproductivity—An overview, in *Productivity of the Ocean: Present and Past, Dahlem Workshop on Productivity of the Ocean; Present and Past. Bath*, edited by W. H. Berger, V. S. Smetacek, and G. Wefer, pp. 1–34, Wiley, Chichester.

Bhushan, R., K. Dutta, and B. L. K. Somayajulu (2001), Concentrations and burial fluxes of organic and inorganic carbon on the eastern margins of the Arabian Sea, *Mar. Geol.*, *178*, 95–113.

Boyer, T. P., J. I. Antonov, O. K. Baranova, H. E. Garcia, D. R. Johnson, R. A. Locarnini , A. V. Mishonov, D. Seidov, I. V. Smolyar, and M. M. Zweng, (2009), World ocean database 2009, in *NOAA Atlas NESDIS 66*, edited by S. Levitus, 216 pp., U.S. Government Printing Office, Washington, D. C.

Brumsack, H. J. (1989), Geochemistry of recent TOC-rich sediments from the Gulf of California and the Black Sea, *Geol. Rundsch.*, *78*, 851–882.

Cai, Y., H. Zhang, H. Cheng, Z. An, R. L. Edwards, X. Wang, L. Tan, F. Liang, J. Wang, and M. Kelly (2012), The Holocene Indian monsoon variability over the southern Tibetan Plateau and its teleconnections, *Earth Planet. Sci. Lett.*, *335*, 135–144.

Calvert, S. E., and T. F. Pedersen (1993), Geochemistry of oxic and anoxic sediments: Implications for the geological record, *Mar. Geol.*, *113*, 67–88.

Calvert, S. E., T. F. Pedersen, P. D. Naidu, and U. Von Stackelberg (1995), On the organic carbon maximum on the continental slope of the Eastern Arabian Sea, *J. Mar. Res.*, *53*, 269–296.

Canfield, D. E. (1994), Factors influencing organic carbon preservation in marine sediments, *Chem. Geol.*, *114*, 315–329.

Cheng, H., D. Fleitmann, R. L. Edwards, X. Wang, F. W. Cruz, A. S. Auler, A. Mangini, Y. Wang, X. Kong, and S. J. Burns (2009), Timing and structure of the 8.2 kyr BP event inferred from ^{18}O records of stalagmites from China, Oman, and Brazil, *Geology*, *37*, 1007–1010.

Chevalier, M., S. Brewer, and M. C. Brian (2017), Qualitative assessment of PMIP3 rainfall simulations across the eastern African monsoon domains during the mid-Holocene and the Last Glacial Maximum, *Quat. Sci. Rev.*, *156*, 107–120.

Clemens, S., W. L. Prell, W. R. Howard (1987), Retrospective dry bulk density estimates from southeast Indian Ocean sediments: comparison of water loss and chloride ion methods, *Mar. Geol.*, *76*, 57–69.

Clemens, S., W. L. Prell, D. Murray, G. B. Shimmield, and G. Weedon (1991), Forcing mechanisms of the Indian Ocean monsoon, *Nature*, *353*, 720–725.

Craig, H., and L. I. Gordon (1965), Deuterium and oxygen-18 variations in the ocean and marine atmosphere, in *Stable Isotopes in Oceanographic Studies and Paleotemperatures, Proceedings of the Spoleto Conference*, edited by E. Tongiorgi, pp. 9–130, Laboratorio di Geologia Nucleare, Pisa, Italy.

Demaison, G. J., and G. T. Moore (1980), Anoxic environments and oil source bed genesis, *Am. Assoc. Pet. Geol. Bull.*, *64*, 1179–1209.

deMenocal, P., J. Ortiz, T. Guilderson, and M. Sarnthein (2000) Coherent high and low-latitude climate variability during the Holocene warm period, *Science*, *288*, 2198–2202.

Dow, W. G. (1978), Petroleum source beds on continental slopes and rises, *Am. Assoc. Pet. Geol. Bull.*, *62*, 1584–1606.

Fleitmann, D., S. J. Burns, M. Mudelsee, U. Neff, J. Kramers, A. Mangini, and A. Matter (2003), Holocene forcing of the Indian monsoon recorded in a stalagmite from southern Oman, *Science*, *300*, 1737–1739.

Fontugne, M. R., and J. C. Duplessy (1986), Variations of the monsoon regime during the Upper Quaternary: Evidence from carbon isotopic record of organic matter in North Indian Ocean sediment cores, *Palaeogeogr. Palaeoclimatol. Palaeoecol.*, *56*, 69–88, doi:10.1016/0031-0182(86)90108-2.

Gallego-Torres, D., F. Martinez-Ruiz, G. J. De Lange, F. J. Jimenez-Espejo, and M. Ortega-Huertas (2010), Trace-elemental derived paleoceanographic and paleoclimatic conditions for Pleistocene Eastern Mediterranean sapropels, *Palaeogeogr. Palaeoclimatol. Palaeoecol.*, *293*, 76–89.

Gasse, F., F. Chalié, A. Vincens, M. A. Williams, and D. Williamson (2008), Climatic patterns in equatorial and southern Africa from 30000 to 10000 years ago reconstructed from terrestrial and near-shore proxy data, *Quat. Sci. Rev.*, *27*, 2316–2340.

Govil, P., and P. D. Naidu (2011), Variations of Indian monsoon precipitation during the last 32 kyr reflected in the surface hydrography of the Western Bay of Bengal, *Quat. Sci. Rev.*, *30*, 3871–3879.

Gupta, A. K., M. Das, and D. M. Anderson (2005), Solar influence on the Indian summer monsoon during the Holocene, *Geophys. Res. Lett.*, *32*, L17703, doi:10.1029/2005GL022685.

Hallberg, R. O. (1976), A geochemical method for investigation of paleoredox conditions in sediments, *Ambio Spec. Rep.*, *4*, 139–147.

Hedges, J. I., and R. G. Keil (1995), Sedimentary organic-matter preservation—An assessment and speculative synthesis, *Mar. Chem.*, *49*, 81–115.

Heggie, D., and T. Lewis (1984), Cobalt in pore waters of marine sediments, *Nature*, *311*, 453–455.

Helly, J. J., and L. A. Levin (2004), Global distribution of naturally occurring marine hypoxia on continental margins, *Deep Sea Res., Part I*, *51*, 1159–1168.

Jiang, D., X. Lang, Z. Tian, and L. Ju (2013), Mid-Holocene East Asian summer monsoon strengthening: Insights from Paleoclimate Modeling Intercomparison Project (PMIP) simulations, *Palaeogeogr. Palaeoclimatol. Palaeoecol.*, *369*, 422–429.

Jones, B., and D. A. Manning (1994), Comparison of geochemical indices used for the interpretation of palaeoredox conditions in ancient mudstones, *Chem. Geol.*, *111*, 111–129.

Joussaume, S., et al. (1999), Monsoons changes for 6000 years ago: Results of 18 simulation from the Paleoclimate Modeling Intercomparison Project (PMIP), *Geophys. Res. Lett.*, *26*, 859–862.

Kessarkar, P. M., and V. P. Rao (2007), Organic carbon in sediments of the southwestern margin of India: Influence of productivity and monsoon variability during the Late Quaternary, *J. Geol. Soc. India*, *69*, 42–52.

Kessarkar, P. M., V. P. Rao, S. W. A. Naqvi, A. R. Chivas, and T. Saino (2010), Fluctuations in productivity and denitrification in the southeastern Arabian Sea during the Late Quaternary, *Curr. Sci.*, *99*, 485–491.

Kessarkar, P. M., V. P. Rao, S. W. A. Naqvi, and S. G. Karapurkar (2013), Variation in the Indian summer monsoon intensity during the Bølling-Allerød and Holocene, *Paleoceanography*, *28*, 413–425.

Laskar, A. H., M. G. Yadava, R. Ramesh, V. J. Polyak, and Y. Asmerom (2013), A 4 kyr stalagmite oxygen isotopic record of the past Indian Summer Monsoon in the Andaman Islands, *Geochem. Geophys. Geosyst.*, *14*, 3555–3566, doi:10.1002/ggge.20203.

Lückge, A., H. D. Rolinski, A. A. Khan, H. Schulz, and U. von Rad (2001), Monsoonal variability in the northeastern Arabian Sea during the past 5000 years: Geochemical evidence from laminated sediments, *Palaeogeol. Palaeoclimatol. Palaeoecol.*, *167*, 273–286.

McIntyre, A., and B. Molfino (1996), Forcing of Atlantic equatorial and subpolar millennial cycles by precession, *Science*, *274*, 1867–1870.

Molfino, B., and A. McIntyre (1990), Precessional forcing of nutricline dynamics in the Equatorial Atlantic, *Science*, *249*, 766–769.

Morford, J. L., and S. Emerson (1999), The geochemistry of redox-sensitive trace metals in sediments, *Geochim. Cosmochim. Acta*, *63*, 1735–1750.

Muller, P. J., and E. Suess (1979), Productivity, sedimentation rate and sedimentary organic carbon in the ocean-organic carbon preservation, *Deep Sea Res., Part A*, *26*, 1347–1362.
Naik, S. S., S. P. Godad, P. D. Naidu, M. Tiwari, and A. L. Paropkari (2014), Early-to late-Holocene contrast in productivity, OMZ intensity and calcite dissolution in the eastern Arabian Sea, *Holocene*, *24*, 749–755.
Nair, R. R., V. Ittekkot, S. J. Manganini, V. Ramaswamy, B. Haake, E. T. Degens, B. N. Desai, and S. Honjo (1989), Increased particle flux to the deep ocean related to monsoons, *Nature*, *338*, 749–751.
Narayana, A. C., P. D. Naidu, N. Shinu, P. Nagabhushanam, and B. S. Sukhija (2009), Carbonate and organic carbon content changes over last 20 ka in the southeastern Arabian Sea: Paleoceanographic implications, *Quat. Int.*, *206*, 72–77.
Naqvi, S. W. A. (1987), Some aspects of the oxygen-deficient conditions and denitrification in the Arabian Sea, *J. Mar. Res.*, *45*, 1049–1072.
Naqvi, S. W. A., H. Naik, D. A. Jayakumar, D. A., M. S. Shailaja, and P. V. Narvekar (2006), Seasonal oxygen deficiency over the western continental shelf of India, in *Past and Present Water Column Anoxia*, edited by L. N. Neretin, pp. 195–224, Springer, Dordrecht.
Paropkari, A. L., S. D. Iyer, O. S. Chauhan, and C. B. Prakash (1991), Depositional environments inferred from variations of calcium carbonate, organic carbon and sulfide sulfur: A core from the southeastern Arabian Sea, *Geo-Mar. Lett.*, *11*, 96–102.
Pattan, J. N., and N. J. G. Pearce (2009), Bottom water oxygenation history in southeastern Arabian Sea during the past 140 ka: Results from redox-sensitive elements, *Palaeogeogr. Palaeoclimatol. Palaeoecol.*, *280*(3–4), 396–405.
Pattan, J. N., T. Masuzawab, P. Divakar Naidu, G. Parthiban, and M. Yamamoto (2003), Productivity fluctuations in the southeastern Arabian Sea during the last 140 ka, *Palaeogeogr. Palaeoclimatol. Palaeoecol.*, *193*, 575–590.
Pattan, J. N., T. Masuzawa, and M. Yamamoto (2005), Variations in terrigenous sediment discharge in a sediment core from southeastern Arabian Sea during the last 140 ka, *Curr. Sci.*, *89*, 1421–1425.
Paulmier, A., D. Ruiz-Pino, and V. Garçon (2011), CO_2 maximum in the oxygen minimum zone (OMZ), *Biogeosciences*, *8*, 239–252.
Peterson, L. C., and W. L. Prell (1985), Carbonate dissolution in the recent sediments of eastern equatorial Indian Ocean: Preservation patterns and carbonate loss above the lysocline, *Mar. Geol.*, *64*, 259–290.
Pokras, E. M., and A. C. Mix (1987), Earth's precession cycle and Quaternary climatic change in tropical Africa, *Nature*, *326*, 486–487.
Prasad, S., et al. (2014), Prolonged monsoon droughts and links to Indo-Pacific warm pool: A Holocene record from Lonar Lake, central India, *Earth Planet. Sci. Lett.*, *391*, 171–182.
Qasim, S. Z. (1977), Biological productivity of the Indian Ocean, *Indian J. Mar. Sci.*, *6*, 122–137.
Radhakrishna, K. (1969), Primary productivity studies in the shelf waters off Alleppey, south-west India, during the post-monsoon, 1967, *Mar. Biol.*, *4*, 174–181.
Ramesh, R., S. K. Bhattacharya, and K. Gopalan (1985), Dendroclimatological implications of isotope coherence in trees from Kashmir Valley, India, *Nature*, *317*, 802–804.
Reichart, G. J., M. den Dulk, H. J. Visser, C. H. van der Weijden, and W. J. Zachariasse (1997), A 225 kyr record of dust supply, paleoproductivity and the oxygen minimum zone from the Murray Ridge (northern Arabian Sea), *Palaeogeogr. Palaeoclimatol. Palaeoecol.*, *134*(1–4), 149–169, doi:10.1016/S0031-0182(97)00071-0.
Riquier, L., N. Tribovillard, O. Averbuch, X. Devleeschouwer, and A. Riboulleau (2006), The Late Frasnian Kellwasser horizons of the Harz Mountains (Germany): Two oxygen-deficient periods resulting from different mechanisms, *Chem. Geol.*, *233*, 137–155.
Russell, J. M., T. C. Johnsan, and M. R. Talbot (2003), A 725 yr cycle in the climate of central Africa during the late Holocene, *Geology*, *31*(8), 677–680.
Saraswat, R., R. Nigam, S. Weldeab, A. Mackensen, and P. D. Naidu (2005), A first look at past sea surface temperatures in the equatorial Indian Ocean from Mg/Ca in foraminifera, *Geophys. Res. Lett.*, *32*, L24605, doi:10.1029/2005GL024093.
Saraswat, R., R. Nigam, A. Mackensen, and S. Weldeab (2012), Linkage between seasonal insolation gradient in the tropical northern hemisphere and the sea surface salinity of the equatorial Indian Ocean during the last glacial period, *Acta Geol. Sin.*, *86*, 1265–1275.
Saraswat, R., D. W. Lea, R. Nigam, A. Mackensen, and D. K. Naik (2013), Deglaciation in the tropical Indian Ocean driven by interplay between the regional monsoon and global teleconnections, *Earth Planet. Sci. Lett.*, *375*, 166–175.
Saraswat, R., D. K. Naik, R. Nigam, and A. S. Gaur (2016), Timing, cause and consequences of mid-Holocene climate transition in the Arabian Sea, *Quat. Res.*, *86*, 162–169.
Sarkar, A., R. Ramesh, B. L. K. Somayajulu, R. Agnihotri, A. J. T. Jull, and G. S. Burr (2000), High-resolution Holocene monsoon record from the eastern Arabian Sea, *Earth Planet. Sci. Lett.*, *177*, 209–218.
Sarkar, S., S. K. Bhattacharya, and M. M. Sarin (1993), Geochemical evidence for anoxic deep water in the Arabian Sea during the last glaciation, *Geochim. Cosmochim. Acta*, *57*, 1009–1016.
Schott, F. A., S. P. Xie, and J. P. McCreary Jr. (2009), Indian Ocean circulation and climate variability, *Rev. Geophys.*, *47*, RG1002, doi:10.1029/2007RG000245.
Schulz, H., U. von Rad, and H. Erlenkeuser (1998), Correlation between Arabian Sea and Greenland climate oscillations of the past 110,000 years, *Nature*, *393*, 54–57.
Shetye, S. R., and A. D. Gouveia (1998), Coastal circulation in the North Indian Ocean. Coastal segment (14, S-W), in *The Sea*, edited by A. R. Robinson and K. H. Brink KH, vol. 11, pp. 523–556, John Wiley, New York.
Singh, A. D., S. J. A. Jung, K. Darling, R. Ganeshram, T. Ivanochko, and D. Kroon (2011), Productivity collapses in the Arabian Sea during glacial cold phases, *Paleoceanography*, *26*, PA3210, doi:10.1029/2009PA001923.
Sinha, A., K. G. Cannariato, L. D. Stott, H. C. Li, C. F. You, H. Cheng, R. L. Edwards, and I. B. Singh (2005), Variability of southwest Indian summer monsoon precipitation during the Bølling-Allerød, *Geology*, *33*, 813–816.
Somayajulu, B. L. K., R. Bhushan, A. Sarkar, G. S. Burr, and A. J. T. Jull (1999), Sediment deposition rates on the Continental margins of eastern Arabian Sea using 210-Pb, 137-Cs and 14-C, *Sci. Total Environ.*, *237–238*, 429–439.
Swallow, J. C. (1984), Some aspects of the physical oceanography of the Indian Ocean, *Deep Sea Res., Part A*, *31*, 693–650.
Thamban, M., V. P. Rao, and S. V. Raju (1997), Controls on organic carbon distribution in sediments from the eastern Arabian Sea Margin, *Geo-Mar. Lett.*, *17*, 220–227.
Thamban, M., V. P. Rao, R. R. Schneider, and P. M. Grootes (2001), Glacial to Holocene fluctuations in hydrography and productivity along the southwestern continental margin of India, *Palaeogeogr. Palaeoclimatol. Palaeoecol.*, *165*, 113–127, doi:10.1016/S0031-0182 (00)00156.
Tiwari, M., R. Ramesh, B. L. K. Somayajulu, A. J. T. Jull, and G. S. Burr (2006), Paleomonsoon precipitation deduced from a sediment core from the equatorial Indian Ocean, *Geo-Mar. Lett.*, *26*, 23–30.
Tiwari, M., R. Ramesh, R. Bhushan, M. S. Sheshshayee, B. L. K. Somayajulu, A. J. T. Jull, and G. S. Burr (2010), Did the Indo-Asian summer monsoon decrease during the Holocene following insolation?, *J. Quat. Sci.*, *25*, 1179–1188, doi:10.1002/jqs.1398.
Tiwari, M., S. S. Nagoji, and R. Ganeshram (2015a), Multi-centennial scale SST and Indian summer monsoon precipitation variability since mid-Holocene and its nonlinear response to solar activity, *Holocene*, *25*, 1–10, doi:10.1177/0959683615585840.

Tiwari, M., A. K. Singh, and D. K. Sinha (2015b), Stable isotopes: Tools for understanding past climatic conditions and their applications in chemostratigraphy, in *Chemostratigraphy*, edited by M. Ramkumar, pp. 65–92. Elsevier Inc., United States.

Tribovillard, N., T. J. Algeo, T. Lyons, and A. Ribaulleau (2006), Trace metals as paleoredox and paleoproductivity proxies: An update, *Chem. Geol.*, *232*, 12–32.

von Rad, U., H. Schulz, V. Reich, M. Den Dulk, U. Berner, and F. Sirocko (1999a), Multiple monsoon-controlled breakdown of oxygen-minimum conditions during the past 30,000 years documented in laminated sediments off Pakistan, *Palaeogeogr. Palaeoclimatol. Palaeoecol.*, *152*, 129–161.

von Rad, U., M. Schaaf, K. H. Michels, H. Schulz, W. H. Berger, and F. Sirocko (1999b), A 5000-yr record of climate change in varved sediments from the oxygen minimum zone off Pakistan, Northeastern Arabian sea, *Quat. Res.*, *51*, 39–53.

Wang, B., J. Liu, H.-J. Kim, P. J. Webster, and S.-Y. Yim (2012), Recent change of the global monsoon precipitation (1979–2008), *Clim. Dyn.*, *39*, 1123–1135.

Wang, Y., H. Cheng, R. L. Edwards, X. Kong, X. Shao, S. Chen, J. Wu, X. Jiang, X. Wang, and Z. An (2008), Millennial and orbital-scale changes in the East Asian monsoon over the past 224,000 years, *Nature*, *451*, 1090–1093.

Webster, P. J. (1987), The variable and interactive monsoon, in *Monsoons*, edited by J. S. Fein and P. L. Stephens, pp. 269–330, John Wiley, New York.

Wedepohl, K. H. (1971), Environmental influences on chemical composition of shales and clays, in *Physics and Chemistry of the Earth*, edited by L. H. Ahrens, F. Press, S. K. Runcorn and H. C. Urey, vol. 8, pp. 307–331, Pergamon, Oxford.

Weldeab, S., D. W. Lea, R. R. Schneider, and N. Andersen (2007), 155000 years of West African monsoon and ocean thermal evolution, *Science*, *316*, 1303–1307.

Wyrtki, K. (1971), *Oceanographic Atlas of the International Indian Ocean Expedition*, pp. 531, Natl. Sci. Found., Washington, D. C.

Yadav, R. R. (2013), Tree ring-based seven-century drought records for the Western Himalaya, India, *J. Geophys. Res. Atmos.*, *118*, 4318–4325, doi:10.1002/jgrd.50265.

Yadava, M. G., and R. Ramesh (2005), Monsoon reconstruction from radiocarbon dated tropical Indian speleothems, *Holocene*, *15*, 48–59.

Yuan, D., H. Cheng, R. L. Edwards, C. A. Dykoski, M. J. Kelly, M. Zhang, J. Qing, Y. Lin, Y. Wang, and J. Wu (2004), Timing, duration, and transitions of the last interglacial Asian monsoon, *Science*, *304*, 575–578.

Zhang, J., F. Chen, J. A. Holmes, H. Li, X. Guo, J. Wang, S. Li, Y. Lü, Y. Zhao, and M. Qiang (2011), Holocene monsoon climate documented by oxygen and carbon isotopes from lake sediments and peat bogs in China: A review and synthesis, *Quat. Sci. Rev.*, *30*, 1973–1987.

Ziegler, M., E. Tuenter, and L. J. Lourens (2010), The precession phase of the boreal summer monsoon as viewed from the eastern Mediterranean (ODP Site 968), *Quat. Sci. Rev.*, *29*, 1481–1490.